Journal of Power Sources, 42 (1993) 55–70

Pulsed-current formation of tetrabasic lead sulfate in cured lead/acid battery plates

L. T. Lam*, H. Ozgun, L. M. D. Cranswick and D. A. J. Rand
CSIRO, Division of Mineral Products, P.O. Box 124, Port Melbourne, Vic. 3207 (Australia)

Abstract

The formation of cured lead/acid battery plates containing a high level (65 wt.%) of tetrabasic lead sulfate (4BS) has been evaluated under both invariant- and pulsed-current conditions. Prior to formation, the plates are subjected to either a short or a long soaking period. The mechanism of formation is dependent on the duration of this treatment. After a short soaking time (30 min), the 4BS is converted to PbO_2 via $PbSO_4$. By contrast, after a long soaking period (15 h), oxidation of 4BS and $PbSO_4$ can proceed simultaneously and produce a high incidence of large voids within the resulting PbO_2 agglomerates. Each of these two mechanisms is unaffected by the waveform of the applied current. Nevertheless, there is a noticeable change in the morphology of the PbO_2 itself. Anhedral particles are produced under invariant-current conditions, whilst well-defined acicular crystals are obtained with pulsed current, particularly at low duty cycles. Irrespective of the soaking period and the corresponding formation mechanism, pulsed current is more efficient in oxidizing 4BS to PbO_2.

Background to study

The manufacture of positive plates for lead/acid batteries involves a sequence of process stages of considerable physicochemical complexity, namely: paste mixing; machine pasting; curing and drying; formation. Large elongated, prismatic crystals of tetrabasic lead sulfate ($4PbO \cdot PbSO_4 = 4BS$) are produced when the pasted plate is cured under conditions of high temperature and high relative humidity (r.h.), i.e., ~80 °C/100% r.h. These crystals form a network within a matrix of fine particles (mainly unreacted lead oxide, PbO). The 4BS-curing route is favoured in the manufacture of deep-cycling batteries as it produces a robust, crystalline network that serves to increase the mechanical strength of the plate material (i.e., in a manner similar to the action of steel rods or wires in reinforced concrete). The inherent interlocking structure is not destroyed during the subsequent formation stage. In effect, the 4BS is converted (through solid-state phase changes or metasomatic processes [1]) into a large number of fine PbO_2 crystals that gather into porous agglomerates [2] and mimic the overall shape of the precursor 4BS crystals. Pavlov and Bashtavelova [3, 4] have formulated a general description for the positive active material. It is suggested that the material consists of small crystals that are grouped into porous agglomerates (the 'microstructure') and then are linked together to form a macroporous network or skeleton (the

*Author to whom correspondence should be addressed.

0378-7753/93/$6.00

'macrostructure'). The latter is considered to impart cycling capability to the plates. The proven ability of 4BS to enhance plate cycle life is consistent with this hypothesis.

From studies with practical batteries, Pierson [5] found that the surface of 4BS-rich plates formed more rapidly than that of plates cured via the tribasic lead sulfate ($3PbO \cdot PbSO_4 \cdot H_2O = 3BS$) route. Subsequent optical micrographs revealed, however, that the interiors of the 4BS crystals had remained largely unconverted. The author had obtained similar results from an earlier microscopic investigation of the *in situ* formation of plate samples [6]. As a result of incomplete formation, the initial capacity of 4BS-based plates is generally lower than expected, but will build up with cycling due to the progressive conversion of the inner parts of the 4BS crystals to PbO_2. Biagetti and Weeks [7] studied the formation of plates prepared from a water paste of chemically-produced 4BS in practical battery acid solutions (1.050 to 1.250 sp. gr. H_2SO_4). The formation was inefficient and this was attributed to the slow oxidation of a substantial, dense layer of $PbSO_4$ that had developed on the surface of the plate. It was further argued that the conversion of this layer is retarded by the oxidation of OH^- ions to oxygen that occurs concurrently at the same potential [8]. This inefficiency problem can be overcome [9] by forming the plates in acid solutions of low gravity (i.e., 1.001 to 1.005 sp. gr.). Under such conditions, the thickness of the sulfation layer is reduced and the oxidation efficiency is almost 100%.

Recently, a mechanism for the oxidation of 4BS crystals to PbO_2 at the microstructural level has been advanced by Pavlov and Bashtavelova [10]. It is argued that the formation of 4BS-cured plates proceeds at different locations: initially, at the individual $PbSO_4$ and 4BS crystals and, later, at the interface between 4BS and the PbO_2 product. According to this mechanism, and the earlier studies of Yarnell and Weeks [9], the rate of the formation process is determined by the mass transport of H^+, SO_4^{2-} and H_2O between the bulk of the solution and the reactive sites.

In the work reported here, an attempt has been made to improve the rate of formation of 4BS-cured plates through the application of a square-pulsed current of constant amplitude. This technique is considered to offer promising results as it is well known to be effective in increasing the rates of reactions that are subject to mass-transport control.

Pulsed-current electrolysis

In simple terms, a pulsed-current generator consists of a rectifier, a switching circuit, and a current monitor (Fig. 1(a)). The current can only flow through the circuit when the switch is closed, i.e., during the 'on-time'. Conversely, there is no current output when the switch is open, i.e., during the 'off-time'. A current profile (i.e., a pulsed current) is obtained when the switching reaction is repeated continuously (Fig. 1(b)). Under these conditions, the following parameters can be defined.

(i) Period, T.

$$T = t_{on} + t_{off} \tag{1}$$

where t_{on} and t_{off} are the on-time and off-time, respectively. The period is the duration of one cycle.

(ii) Duty cycle, θ.

$$\theta = t_{on}/T \tag{2}$$

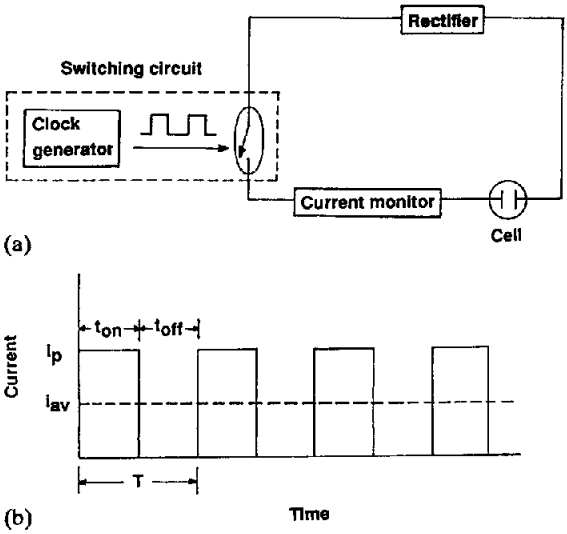

Fig. 1. Schematic diagram of (a) pulse generator; (b) pulsed-current waveform.

The duty cycle relates to the proportion of time in each period that current is passed through the circuit.

(iii) Average current, i_{av}.
The average current, i_{av}, is equivalent to the invariant current that gives, during one period, the same quantity of charge as that produced by the pulsed current of amplitude i_p, i.e.,

$$i_{av} \times T = i_p \times t_{on} \tag{3}$$

Therefore, it follows that:

$$i_{av} = i_p \times t_{on}/T = i_p \times \theta \tag{4}$$

This demonstrates the greater flexibility of the pulsed-current approach — three variables (i.e., current amplitude, on-time and off-time) can now assist the search for optimization of the formation process compared with the availability of only one parameter (i.e., current amplitude) in the invariant-current method. Pulsed-current electrolysis has been applied widely in metal-deposition studies, e.g., in the plating of cobalt, copper, gold, nickel, silver, tin, zinc [11–20]. As early as 1910, a theoretical analysis of mass transport under pulsed, reversed or alternating current electrolysis was undertaken by Rosebrugh and Miller [21]. Much later, a simple diffusion model was developed [22–25] to calculate the rate of metal deposition under pulsed-current electrolysis. The influence of the pulsed-current parameters on the faradaic process has been investigated by Puippe and Ibl [26]. By contrast, very little attention has been directed towards the use of the pulsed-current technique for the formation of lead/acid battery plates. (Note, however, there have been several investigations, e.g., [27–30], of the effects of pulsed-current on the discharge behaviour of lead/acid batteries. These have been promoted by the development of chopper devices for motor-speed control in electric vehicles.)

One of the most important advantages of pulsed electrolysis is the enhancement of mass transport during the off-time of the pulsed cycle. Under suitable conditions,

a high instantaneous current can be applied without initiation of a second, and perhaps undesirable, reaction (e.g., oxygen evolution). Therefore, for lead/acid batteries manufactured via the 4BS-curing route, pulsed current is expected to increase the plate-formation rate by acceleration of the normally slow diffusion of ion species from the bulk of solution to the plates and, correspondingly, into the large 4BS crystals.

Experimental

Plate preparation

Paste was made by combining Barton-pot leady oxide, sulfuric acid solution and water in the proportions given in Table 1. The resulting mixture had a density of 4.1 g cm^{-3}.

After mixing, the paste was applied, by hand, to Pb–1.7 wt.% Sb grids (dimensions: 150 mm (width) × 100 mm (length) × 1.8 mm (thickness)) and then compacted under the weight of a purpose-built, stainless-steel roller. The pasted plates were mounted, 8 mm apart, on a rack and placed in a petri dish. The latter contained a small amount of distilled water and was enclosed by a glass beaker. Curing was conducted at 90 °C/100% r.h. for 10 h, followed by 40 °C/ambient humidity for a further 14 h. The initial high level of humidity was achieved by evaporation of the distilled water reservoir. The resulting cured plates had a nominal *C*/20 discharge capacity of ~10 A h/plate.

Plate formation

Each test cell comprised six positive and seven negative plates. The positives were enclosed in Daramic envelope separators. The negatives were produced under factory conditions. Sulfuric acid solution (1.250 sp. gr.) was introduced into the cell compartment to give an active-material (g)/acid (cm^3) ratio of 2.21 at 25 °C. The formation was conducted at 25 °C with either invariant or pulsed current after the cured plates had been allowed to stand in the battery acid for either 30 min or 15 h. For pulsed-current formation, a programmable function generator (Wavetek, model 175) was used in conjunction with battery testing equipment that was designed and built in the CSIRO laboratories. A continuous square-pulsed current was delivered to the test cell and the resulting formation current and voltage were monitored on an oscilloscope (BWD Electronics, model 820).

X-ray diffraction phase analysis

Samples of cured and formed materials were subjected to X-ray diffraction (XRD) phase analysis. The X-ray peak intensities were measured by an automated, integrated, step-scan procedure on a standard Philips PW1710 diffractometer that was fitted with a curved graphite monochromator using copper Kα radiation. The data were collected on chart paper for visual examination, as well as stored on computer files for subsequent

TABLE 1

Paste formulation for positive-plate material

Leady oxide (kg)	1091
Water (l)	120
1.4 sp. gr. H_2SO_4 (l)	81
Paste density (g cm^{-3})	4.1

computational analysis. The phase compositions were determined by an advanced XRD method developed in the CSIRO laboratories [31]. The latter uses measurement of the peak height to determine quantitatively the relative proportions of the individual crystalline materials in the samples under study.

Scanning electron microscopy

The morphology of cured and formed materials, taken from mid-way through the thickness of each plate, was examined with a JEOL JSM-25S III scanning electron microscope (SEM). The plate samples were attached to double-sided tape and mounted on a carbon block. A palladium–gold alloy film was sputtered over the entire block to provide satisfactory imaging of the material. The morphology of the plate material was examined by SEM analysis with secondary electron imaging.

For cross-sectional examinations, the samples were impregnated with epoxy resin in a vacuum desiccator. After setting, the mount was polished by hand on successive grades of abrasive paper from 240 up to 1200 grit. Final polishing was performed on a machine (Kent, model 3) with, in sequence, diamond paste of 6, 3 and 1 μm particle size. A carbon film was then deposited over the entire block and the phase distribution in the inner, central region of the chosen sample was observed by SEM analysis with back-scattered electron imaging.

Results and discussion

Phase composition/morphology of 4BS-cured material

Phase analysis showed that the cured material prepared in this study comprised: 65 wt.% 4BS; 21 wt.% α-PbO; 7 wt.% β-PbO; 7 wt.% 3BS.

After curing, the plate had an orange-coloured surface and a dark-green interior. Secondary electron micrographs (Fig. 2) revealed that the latter consisted of large, square-prismatic 4BS crystals with lengths up to 40 μm. It was also found that the surface of the crystals exhibited an appreciable number of defects. The average length of the 4BS crystals was shorter, and the surface more defective, than in the case of 4BS prepared for longer periods (e.g., 48 h [32]) under continuous conditions of high

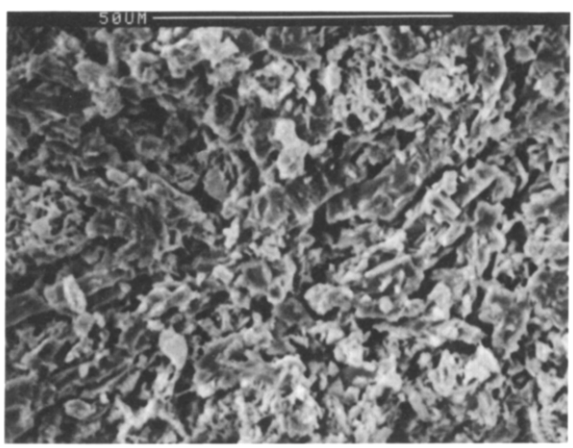

Fig. 2. Secondary electron micrograph of 4BS-cured material. Magnification bar = 50 μm.

temperature and high humidity. These differences are due to the fact that recrystallization (or growth) of 4BS cannot take place during the high-temperature/low-humidity conditions employed in the second stage of the curing schedule used here.

Sulfation of cured plates

In order to determine the influence of the soaking time on the progressive sulfation of cured material, the plates were allowed to stand in the formation acid (1.250 sp. gr. H_2SO_4) for 35 h. The phase composition and morphology of the plate material were evaluated at various intervals during this period by XRD phase analysis and SEM examination, respectively.

The change in phase composition with plate soaking is presented in Fig. 3. During the first hour, there is a marked decrease in both α-PbO and 4BS, and a corresponding rapid increase in $PbSO_4$. With further soaking, the changes in the α-PbO, 4BS and $PbSO_4$ levels slow down and limiting values are reached. The sulfation reaction can be expressed as:

$$4PbO \cdot PbSO_4 + 4H_2SO_4 \longrightarrow 5PbSO_4 + 4H_2O \quad (5)$$

Clearly, H^+ and SO_4^{2-} ions are required to diffuse through the $PbSO_4$ layer to the surface of the 4BS. It is also expected that the movement of these ions will be severely arrested when the thickness of the $PbSO_4$ layer exceeds a certain value. In the present example, this appears to occur after about 25 h of soaking.

Back-scattered electron micrographs (Fig. 4) show that the soaking of cured plates in sulfuric acid causes both the PbO and 4BS crystals to become covered with dense films of $PbSO_4$ (the dark-grey regions in Figs. 4(a)–(c)). The film thickness increases with the soaking time, but eventually levels off to an average value of ~ 3 μm after 25 h (Fig. 5). The limiting amount of $PbSO_4$ is reached at a time that is consistent with the value derived from XRD phase analysis data (cf., Fig. 3). After soaking, all but the largest of the 4BS crystals are converted completely to $PbSO_4$ (Fig. 4(c)).

Phase composition/morphology of 4BS-formed material

As established in earlier studies [6, 32, 33], the formation process of 4BS-cured plates commences at the grid surface and then spreads into the cured material, preferentially via the surface of the 4BS crystalline network. At each 4BS crystal, the oxidation proceeds from the surface towards the interior of the crystal. It should be

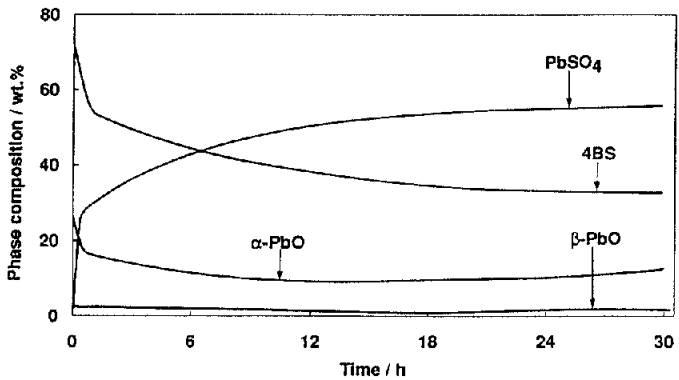

Fig. 3. Phase composition of 4BS-cured plates during soaking in 1.250 sp. gr. H_2SO_4.

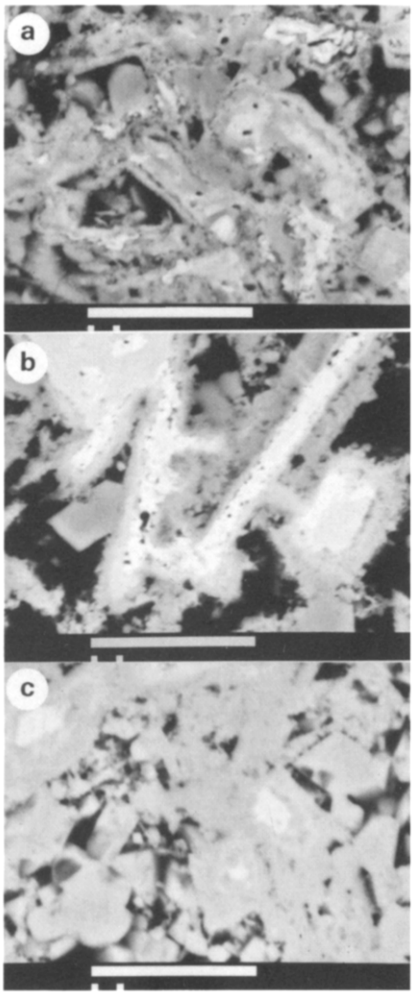

Fig. 4. Back-scattered electron micrographs of polished cross sections of cured material. These show the progressive growth of the sulfation layer around 4BS crystals with soaking time: (a) 6 h; (b) 19 h; (c) 36 h. Magnification bar = 10 μm.

noted, however, that the 4BS crystals become covered by compact films of $PbSO_4$ immediately the formation acid is introduced. During the early stages of formation, these $PbSO_4$ layers develop further into those regions where conversion to PbO_2 has not yet occurred. To determine the effect of differing degrees of $PbSO_4$ encapsulation on formation efficiency, the oxidation of 4BS crystals covered with either a thick or a thin layer of $PbSO_4$ (as promoted by long/short soaking times) has been examined using both invariant and pulsed current.

Long soaking time

The change in phase chemistry and composition during invariant-current (6A) formation is shown in Fig. 6(a). The formation was initiated after the cured plates had been allowed to stand in 1.250 sp. gr. H_2SO_4 for 15 h. It can be seen that this

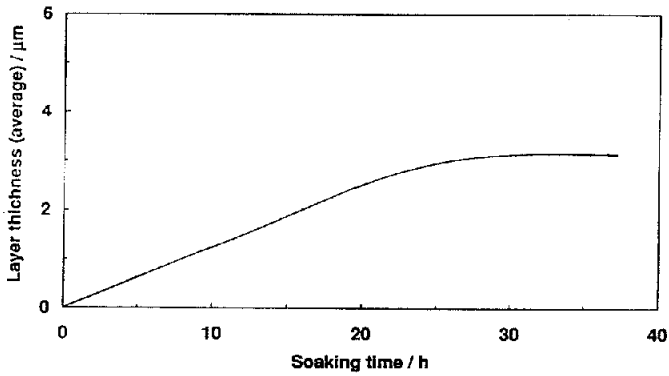

Fig. 5. Development of sulfation layer with time.

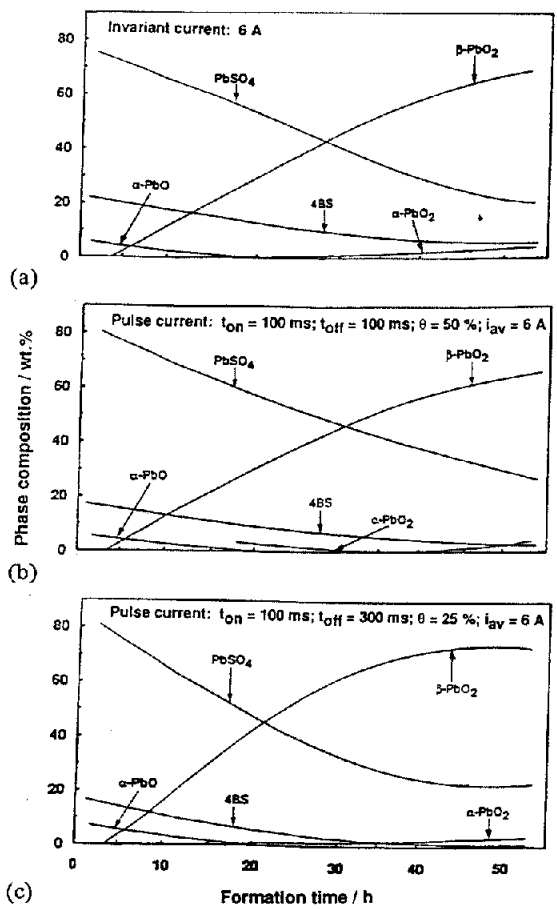

Fig. 6. Phase composition of formed material produced after 15 h soaking: (a) invariant current; (b) and (c) pulsed current.

treatment converts most of the α-PbO and 4BS to $PbSO_4$. During formation, the oxidation of $PbSO_4$ proceeds at a faster rate than that of 4BS. A minor amount of α-PbO_2 is produced at later stages of the process.

Similar results are obtained for pulsed-current formation using an on-time of 100 ms, a duty cycle of 50%, and an average current of 6 A (Fig. 6(b)). By contrast, the level of β-PbO_2 increases more rapidly when the duty cycle is decreased to 25% by increasing the off-time but keeping the other process conditions constant, i.e., on-time 100 ms, average current 6 A (Fig. 6(c)). This suggests that the optimum pulsed-current conditions for 4BS oxidation require a low duty cycle.

The morphology of the active material derived from 4BS-cured plates after a long soaking time is presented in Fig. 7. The active material produced under invariant-current formation is composed mainly of agglomerates of individual, anhedral β-PbO_2

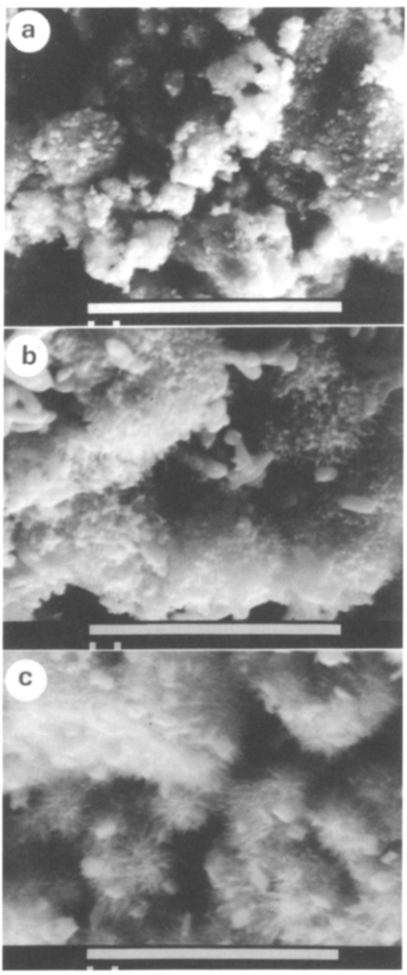

Fig. 7. Secondary electron micrographs of formed material (15 h soaking): (a) invariant current 6 A; (b) pulsed current: average current 6 A, on-time 100 ms, duty cycle 50%; (c) pulsed current: average current 6 A, on-time 100 ms, duty cycle 25%. Magnification bar = 10 μm.

crystals (Fig. 7(a)). Under pulsed-current conditions, there is a change in the morphology of β-PbO_2 towards small, needle-like crystals. The latter become more defined and grow to greater lengths (up to ~ 0.7 μm) when the material is formed with a low duty cycle (Fig. 7(c)). For either type of current profile, remnants of unoxidized $PbSO_4$ crystals are embedded in the PbO_2 agglomerates.

Back-scattered electron micrographs of polished cross sections of the above-mentioned formed materials are shown in Figs. 8 and 9. The structure of the material is similar when produced under the action of either invariant current or pulsed current

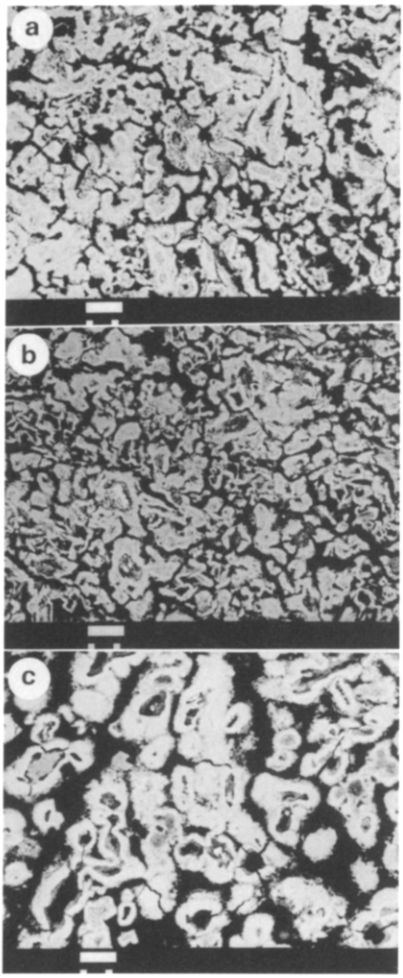

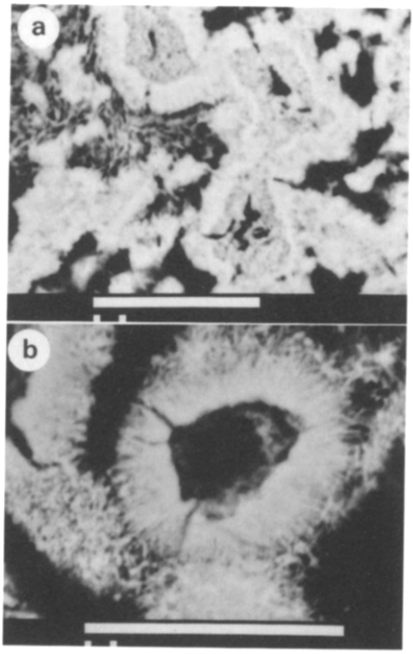

Fig. 8. Back-scattered electron micrographs of polished cross sections of formed material (15 h soaking): (a) invariant current 6 A; (b) pulsed current: average current 6 A, on-time 100 ms, duty cycle 50%; (c) pulsed current: average current 6 A, on-time 100 ms, duty cycle 25%. Magnification bar = 10 μm.

Fig. 9. Back-scattered electron micrographs of polished cross sections of formed material (15 h soaking): (a) invariant current 6 A; (b) pulsed current: average current 6 A, on-time 100 ms, duty cycle 25%. Magnification bar = 10 μm.

with a 50%-duty cycle (Fig. 8(a), (b)). The interiors of the 4BS crystals remain largely unformed. At high magnifications, micrographs reveal that there are large pores running through the oxidized surface layers into the bulk of the 4BS crystals (Fig. 9(a)). It is further found that the inner parts of the crystals have disintegrated into a mixture of particles with different sizes. This process is accompanied by the development of voids. The latter become more prominent when the plates are formed under pulsed current with a 25%-duty cycle; the resulting material contains an appreciable number of PbO_2 agglomerates with hollow centres (Fig. 8(c) and Fig. 9(b)).

Short soaking time

The change in phase composition of formed material prepared with invariant current (6 A) is shown in Fig. 10(a). The formation was commenced after the cured plates were allowed to soak in 1.250 sp. gr. H_2SO_4 for 30 min. As expected, the level of the residual 4BS is greater than that found after a long soaking period (cf., Fig. 6(a)). The results show that the levels of 4BS and α-PbO are virtually unchanged throughout the formation process. By contrast, the $PbSO_4$ content decreases from 45

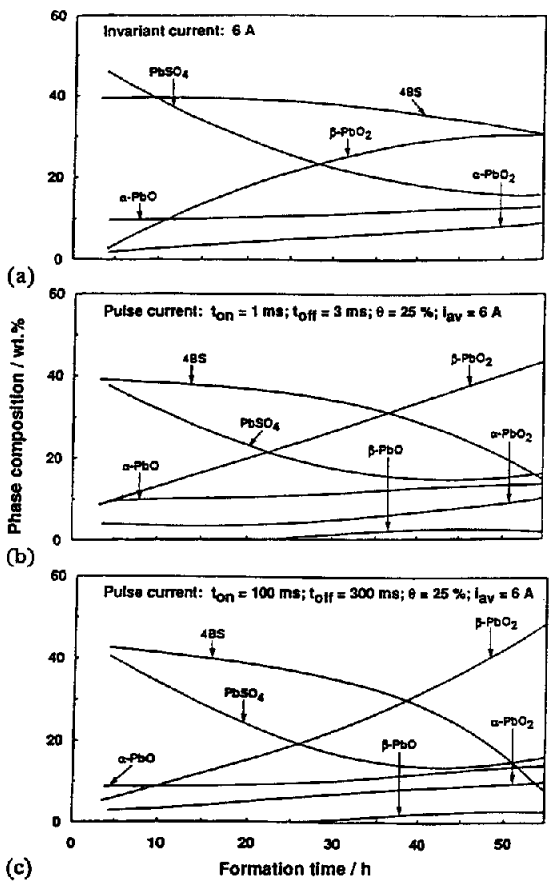

Fig. 10. Phase composition of formed material produced after 30 min soaking: (a) invariant current; (b) and (c) pulsed current.

to 20 wt.% during the first 30 h of formation and then exhibits a slight decrease to a limiting value of ~18 wt.%. Correspondingly, the β-PbO_2 increases rapidly over 30 h and then displays a slight increase over the remaining period of formation. Unlike the behaviour observed after a long soaking period, a small amount of α-PbO_2 develops at an early, rather than at a late, stage of formation.

Figure 10(b) presents the phase composition of formed material obtained under pulsed-current conditions of: on-time 1 ms; duty cycle 25%; average current 6 A. During the first 30 h, the change in composition is similar to that produced by application of an invariant current (cf., Fig. 10(a)). That is: (i) little change in 4BS; (ii) decrease in $PbSO_4$; (iii) increase in β-PbO_2. Beyond this period, however, pulsed current accelerates the conversion of 4BS to β-PbO_2. Curiously, trace amounts of β-PbO are also produced. The yield of β-PbO_2 is enhanced slightly when using the same duty cycle (viz., 25%) but a longer on-time, i.e., 100 ms as opposed to 1 ms, (see Fig. 10(c)).

Secondary electron micrographs reveal that the material is composed mainly of anhedral grains in plates subjected to invariant-current formation (Fig. 11(a)), and of finer, needle-like crystals when the plates are processed under pulsed current (Fig. 11(b) and (c)). (As expected, for a given duty cycle, the acicular nature is more pronounced as the on-time is increased.) This change in crystal habit is similar to that for plates subjected to a long soaking period (cf., Fig. 7). By contrast, back-scattered electron micrographs illustrate clear differences between the interior structure of the crystals in plates formed after long and short soaking periods (cf., Figs. 9 and 12). After short soaking treatment, most of the unformed interiors of the 4BS crystals retain their original geometry and texture (i.e., there is no disintegration of the type observed in plates subjected to a long soaking time. In addition, there is a continuous gap at the boundary between the outer PbO_2 crust and the inner, unconverted 4BS crystal (Fig. 12(c)).

In summary, comparison of the data presented in Figs. 6 and 10 shows that, for the same soaking time, the formation efficiency is greater with the pulsed-current than with the invariant-current technique. Conversely, for the same formation procedure (i.e., either invariant or pulsed current), the oxidation to β-PbO_2 is faster after a long soaking period has been applied.

Mechanism of formation process

From the above results, it can first be concluded that the duration of the soaking treatment influences the mechanism of the formation process. After a long soaking period, conversion of $PbSO_4$ to PbO_2 proceeds from the surface towards the interior of each host 4BS crystal. This is shown schematically in Figs. 13(a) and (b). In some regions, however, the presence of pores allows the inner parts of the 4BS crystals to convert simultaneously to $PbSO_4$ and PbO_2 (Fig. 13(c)). Clearly, the content of $PbSO_4$ will decrease more rapidly relative to that of 4BS; this is in agreement with the phase analysis data given in Fig. 6. Since PbO_2 has a smaller molar volume than 4BS, crystals of the latter will disintegrate into a mixture of PbO_2, $PbSO_4$ and 4BS particles, and will subsequently develop large voids when conversion to PbO_2 is complete (Fig. 13(d)). As pores are frequently found to run through the shells of the 'hollow' crystals, it is expected that the formed material will become fragmented after several charge/discharge cycles of battery operation. Thus, an optimum size/strength of the 4BS crystals should be determined to yield maximum cycle life for battery plates.

There is a lower incidence of pores in the thinner sulfation layer produced on the 4BS crystals after a short soaking period. Consequently, during the initial stages

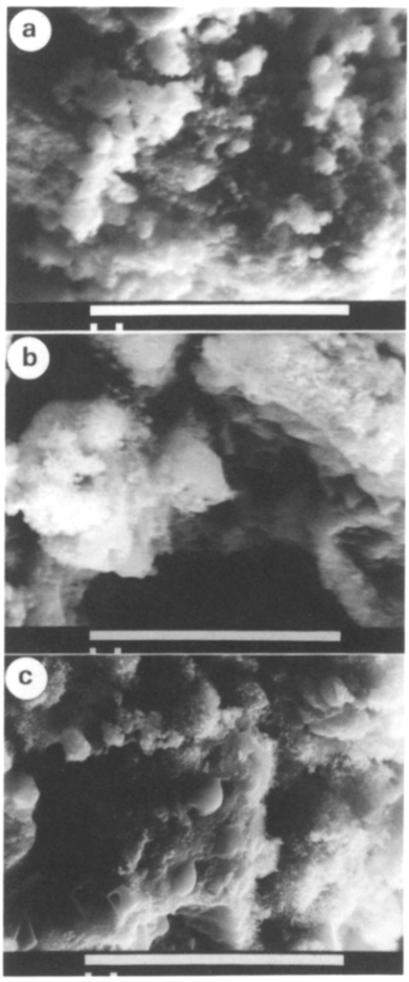

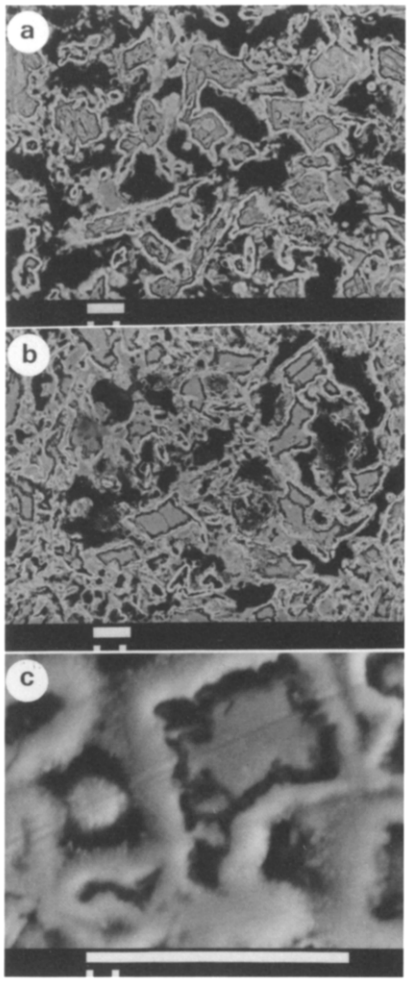

Fig. 11. Secondary electron micrographs of formed material (30 min soaking): (a) invariant current 6 A; (b) pulsed current: average current 6 A, on-time 1 ms, duty cycle 25%; (c) pulsed current: average current 6 A, on-time 100 ms, duty cycle 25%. Magnification bar = 10 μm.

Fig. 12. Back-scattered electron micrographs of polished cross sections of formed material (30 min soaking): (a) invariant current 6 A; (b) pulsed current: average current 6 A, on-time 1 ms, duty cycle 25%; (c) pulsed current: average current 6 A, on-time 100 ms, duty cycle 25%. Magnification bar = 10 μm.

of formation, oxidation takes place almost exclusively in this layer and the 4BS content remains virtually unaffected. This is shown schematically in Figs. 14(a) and (b). In the later stages of formation (i.e., after ~30 h, Fig. 10), there are two possible pathways for further progress of the formation reaction: (i) $PbSO_4$ and 4BS oxidize concurrently in a manner similar to that described above for plates subjected to a long soaking period; (ii) 4BS is converted to $PbSO_4$ (due to the attack from sulfate species released from oxidation of the outer $PbSO_4$ layer), and the latter is subsequently oxidized to PbO_2.

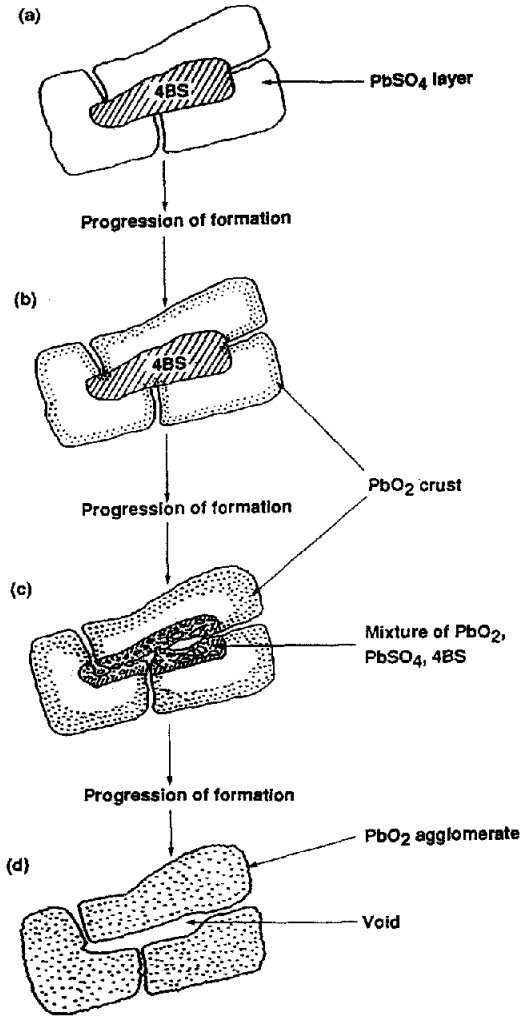

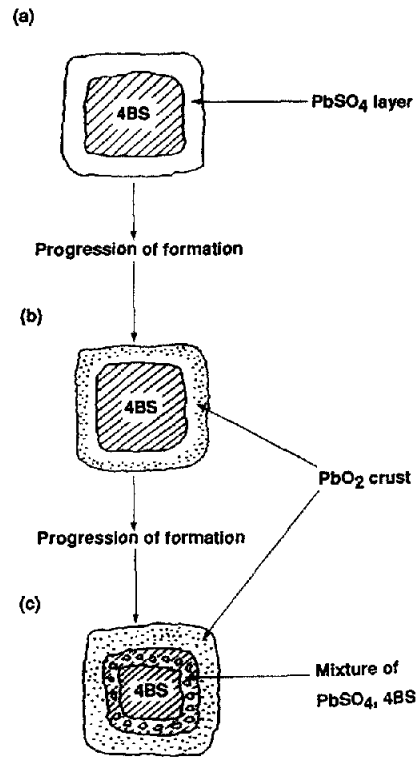

Fig. 13. Schematic diagram of plate formation after long soaking time.

Fig. 14. Schematic diagram of plate formation after short soaking time.

Pathway (i) would result in a concomitant decrease in both the $PbSO_4$ and 4BS content, while pathway (ii), although causing a decrease in 4BS, would produce little change in the level of $PbSO_4$. Since the latter is observed experimentally (Fig. 10), it is reasonable to assume that pathway (ii) is the operative process (see Fig. 14(c)).

As mentioned above, the formation process commences at the grid and moves outwards into the cured material. Since the latter is in contact with acid, sulfate films will continue to grow around those 4BS crystals that are ahead of the oxidation front, i.e., in the outermost (surface) zones of the plate. Thus, pathway (i) may also occur at various locations (in particular, at the surface) in plates that have been subjected to a short soaking treatment. Note, the studies reported here have been conducted

on material taken from the inner regions of the plates where one formation mechanism is expected to predominate.

Value of pulsed-current technique

The oxidation of $PbSO_4$ to PbO_2 proceeds through a dissolution-precipitation mechanism. The reaction can be represented as follows:

$$PbSO_4 \rightleftharpoons Pb^{2+} + SO_4^{2-} \quad (6)$$

$$Pb^{2+} + 2H_2O \longrightarrow PbO_2 + 4H^+ + 2e^- \quad (7)$$

In order for formation to proceed, transport of H^+ and SO_4^{2-} ions, as well as H_2O, is required between the oxidation layer and the bulk of the electrolyte. Difficulties in the movement of these reaction species may regulate the oxidation process. Compared with the conventional formation procedure (i.e., invariant current), the pulsed-current technique gives higher formation efficiency through enhancement of the diffusion of the reaction species during the off-time. A low duty cycle is particularly effective because, for the same on-time, a decrease in the duty cycle is equivalent to an increase in the off-time and this provides greater opportunity for the reaction species to diffuse through the PbO_2 layer.

It should also be noted that both the structure of the formed material as a whole, and the morphology of the PbO_2 itself, are influenced by the flow of Pb^{2+} ions and the concentration of sulfuric acid [34]. Takehara and Kanamura [35] have established that the size of the PbO_2 crystals decreases with increase in acid concentration. As seen from the eqns. (6) and (7), the oxidation of $PbSO_4$ results in generation of H_2SO_4 at the interface with the nascent PbO_2 layer. The concentration of acid at this interface is expected to be higher for plates formed under invariant current as opposed to pulsed current because of the influence of mass-transport processes. Therefore, the size of the PbO_2 particles produced by invariant current should be smaller than those obtained with pulsed current. This influence of the current regime causes a marked difference in PbO_2 morphology: under invariant current, the smaller PbO_2 particles gather together into dense, anhedral agglomerates, whilst under pulsed current the PbO_2 develops as larger, acicular crystals. Further work in our laboratories will examine the subsequent effects of these changes in PbO_2 crystal habit on plate capacity and cycle life.

Concluding remarks

It has been observed that the conversion mechanism of 4BS to PbO_2 is determined by the extent to which the plates have been soaked in acid prior to the formation process. For a given soaking period, the resulting mechanism is independent of whether a pulsed or an invariant current is applied. Nevertheless, pulsed-current conditions do improve the efficiency of the formation process, i.e., a greater proportion of PbO_2 is produced after a given formation time. In addition, there is an accompanying change in PbO_2 morphology that may provide beneficial effects in terms of plate performance in subsequent battery service.

Clearly, the implementation of a pulsed-charging strategy for plate formation would be costly to the battery manufacturer. The results obtained from this study suggest, however, that the pulsed-current technique may offer a promising approach to the rapid charging of lead/acid batteries. The development of an effective and

efficient rapid-charging strategy is a major objective in research programmes aimed at advancing battery performance for electric-vehicle applications.

References

1 J. Burbank, *J. Electrochem. Soc., 113* (1966) 10.
2 D. Pavlov and G. Papazov, *Electrochemical Power Sources First Symp.*, Dum Techniky CVTS, Prague Zari, Czechoslovakia, 1975, p. 49.
3 D. Pavlov and E. Bashtavelova, *J. Electrochem. Soc., 131* (1984) 1468.
4 D. Pavlov and E. Bashtavelova, *J. Electrochem. Soc., 133* (1986) 241.
5 J. R. Pierson, in D. H. Collins (ed.), *Power Sources 2, Research and Development in Non-Mechanical Electrical Power Sources,* Pergamon, Oxford, 1970, p. 103.
6 J. R. Pierson, *Electrochem. Technol., 5* (1967) 323.
7 R. V. Biagetti and M. C. Weeks, *Bell System Tech. J.,* (Sept.) (1970) 1305.
8 D. Pavlov, G. Papazov and V. Iliev, *J. Electrochem. Soc., 119* (1972) 8.
9 C. F. Yarnell and M. C. Weeks, *J. Electrochem. Soc., 126* (1979) 7.
10 D. Pavlov and E. Bashtavelova, *J. Power Sources, 31* (1990) 243.
11 H. Y. Cheh, H. B. Linford and C. C. Wan, *Plat. Surf. Finish., 64* (1977) 66.
12 H. Y. Cheh, P. C. Andricacos and H. B. Linford, *Plat. Surf. Finish., 64* (1977) 42.
13 L. T. Lam, I. Ohno and S. Haruyama, *Denki Kagaku, 51* (1984) 652.
14 P. C. Andricacos, H. Y. Cheh and H. B. Linford, *Plat. Surf. Finish., 64* (1977) 44.
15 T. Shimojo, K. Ando and L. T. Lam, *Met. Finish. Soc. Jpn., 32* (1985) 652.
16 L. T. Lam, I. Ohno, T. Saji and S. Haruyama, *J. Met. Finish. Soc. Jpn, 32* (1981) 64.
17 L. T. Lam, I. Ohno, T. Saji and S. Haruyama, *J. Met. Finish. Soc. Jpn, 33* (1982) 29.
18 L. T. Lam, Fundamental study of pulse plating, *Ph.D. Thesis,* Tokyo Institute of Technology, Japan, Mar. 1982.
19 W. Sullivan, *Plat. Surf. Finish., 62* (1975) 139.
20 E. S. Chen and F. K. Sautter, *Plat. Surf. Finish., 63* (1976) 28.
21 T. R. Rosebrugh and W. L. Miller, *J. Phys. Chem., 14* (1910) 816.
22 H. Y. Cheh, *J. Electrochem. Soc., 118* (1971) 551; *118* (1971) 1132.
23 N. Ibl, *Surf. Technol., 10* (1980) 81.
24 K. I. Popov, M. D. Makimovic and B. M. Ocokoljic, *Surf. Technol., 11* (1980) 99.
25 I. Ohno, L. T. Lam and S. Haruyama, *Denki Kagaku, 51* (1984) 167.
26 J. Cl. Puippe and N. Ibl, *J. Appl. Electrochem., 10* (1980) 775.
27 M. G. Jayne, in D. H. Collins (ed.), *Power Sources 6, Research and Development in Non-Mechanical Electric Power Sources,* Academic Press, London, 1977, p. 35.
28 R. L. Cataldo, *Proc. 13th Intersoc. Energy Conv. Eng. Conf., San Diego, CA, Aug. 20–25, 1978,* p. 764.
29 S. Caulder, A. Simon and E. Dowgiallo, *Proc. 17th Intersoc. Energy Conv. Eng. Conf., Los Angeles, CA, Aug. 8–12, 1982,* p. 616.
30 R. J. Hill, D. A. J. Rand and R. Woods, in L. J. Pearce (ed.), *Power Sources 10, Research and Development in Non-Mechanical Electric Power Sources,* Paul Press, London, 1985, p. 459.
31 R. J. Hill, A.M. Foxworthy and R. J. White, *J. Power Sources, 32* (1990) 315.
32 L. T. Lam, A. M. Vecchio-Sadus, H. Ozgun and D. A. J.Rand, *J. Power Sources, 38* (1992) 87.
33 D. Pavlov, G. Papazov and V. Iliev, *J. Electrochem. Soc., 119* (1972) 8.
34 D. Pavlov and E. Bashtavelova, *J. Power Sources, 30* (1990) 77.
35 Z. Takehara and K. Kanamura, *J. Electrochem. Soc., 134* (1987) 13, 1604.